Macromolecules
ARTICLE

Macromolecules **2010**, *43*, 347–353 **347**
DOI: 10.1021/ma902070h

Anisotropy and Transport in Poly(arylene ether sulfone) Hydrophilic−Hydrophobic Block Copolymers

Jianbo Hou, Jing Li, and Louis A. Madsen*

Department of Chemistry and Macromolecules and Interfaces Institute, Virginia Polytechnic Institute and State University, Blacksburg, Virginia 24061

Received September 16, 2009; Revised Manuscript Received October 31, 2009

ABSTRACT: Designing tailored block copolymers represents a viable strategy for building polymer membranes with fruitful combinations of properties, such as the high ionic or small molecule conductivity and high mechanical strength needed for applications such as fuel cells and reverse-osmosis water purification. Here we present a systematic study of water transport and morphological alignment in a class of poly(arylene ether sulfone) hydrophilic−hydrophobic multiblock copolymer membranes and compare these with Nafion 212. Multiaxis pulsed-field-gradient NMR yields diffusion anisotropy, the ratio of diffusion coefficients measured both in plane ($D_{\|}$) and through plane ($D_{\perp}$), as a function of water uptake and block lengths. As block mass increases, diffusion anisotropy exhibits an increasing dependence on water uptake, in contrast to Nafion 212, where diffusion is isotropic and displays no dependence on water uptake. ^{2}H NMR spectroscopy on absorbed D_2O further probes membrane alignment modes. Both types of measurements corroborate uniformly ordered planar structures oriented through the membrane plane in accordance with a lamellar morphology previously observed locally with microscopy. The combination of these two measurements also provides insights into average defect distributions.

1. Introduction

Ionomer membranes find wide applications in fuel cells and reverse-osmosis water purification.[1,2] Many successful membrane materials consist of hydrophilic and hydrophobic polymer moieties, which phase separate into nanoscale water channels to facilitate the transport of mobile species, such as water molecules and protons. Structural characteristics like orientational ordering and multiscale hierarchical morphologies strongly affect the macroscopic properties and performance of these materials, such as proton conductivity and water transport.[3,4] The current benchmark material for proton exchange membranes (PEM) is Nafion, a commercially available perfluorosulfonate ionomer that has been studied extensively with respect to morphology, water transport, and proton conductivity.[5−10] Such materials exhibit high proton conductivity when absorbing an adequate amount of water. However, their performance in terms of thermal stability, mechanical strength, and proton conductivity decays drastically at elevated temperature, which limits their applications.[11,12] A current goal in fuel cell membrane design is to develop materials that can work efficiently at higher temperature (> 120 °C) and low relative humidity.

Consequently, a class of aromatic-based block copolymers consisting of sharply separated hydrophilic and hydrophobic nanophase-separated morphologies are under development.[12−15] These block copolymers are potential candidates to work at low humidity due to their high water absorption. In addition, these materials show excellent thermal and chemical stabilities,[12] which enable them to work at elevated temperature without degradation in performance. Finally, because of the high cost of perfluorinated membranes (~$2500/kg), these aromatic hydrocarbon materials promise substantially reduced cost in potential wide applications such as fuel cells and other separations applications. Figure 1 shows the structures of Nafion and the BPSH−BPS polymers studied here,[16] where "BP" and "S" correspond to biphenol and sulfonated, respectively. While microscopy is useful for probing local environments, NMR can provide bulk average morphology as well as convenient and reliable molecular (or ion) transport information. Here, we describe NMR measurements probing anisotropy over a range of block lengths and water uptakes in these solution-cast BPSH−BPS multiblock systems and compare them to the benchmark dispersion-cast polymer Nafion 212.

We aim to explore relationships between properties and structures of these materials via studies using pulsed-field-gradient (PFG) NMR diffusometry[17,18] and ^{2}H NMR spectroscopy.[19] Diffusometry is an effective, convenient, and repeatable method that can provide quantitative data on how mobile species diffuse,[20,21] including in ionomer membranes.[3,22−24] Rollet et al. investigated the transport of different ions in sulfonated polyimide ionomers by PFG NMR and radiotracer techniques.[25] They found dramatic diffusion anisotropy of ions in plane vs through plane, where ion diffusion in the former direction was much faster than the latter. Kidena studied proton (water) diffusion anisotropy in Nafion at different temperatures via PFG NMR.[26] According to Kidena measurement results, diffusion anisotropy was observable at low temperature (~0 °C) but was approximately isotropic above room temperature. We recently reported NMR studies of anisotropic structures in several types of Nafion processed under different conditions, based on which we proposed morphological symmetry models.[3]

Our group is among the first to perform correlated studies of local self-diffusion and anisotropy in nanophase-separated polymers in order to understand the fundamental relationship between morphological alignment and transport in these materials. For these NMR experiments (diffusometry and spectroscopy), water molecules act as mobile probes interacting with

*Corresponding author. E-mail: lmadsen@vt.edu.

Published on Web 11/16/2009

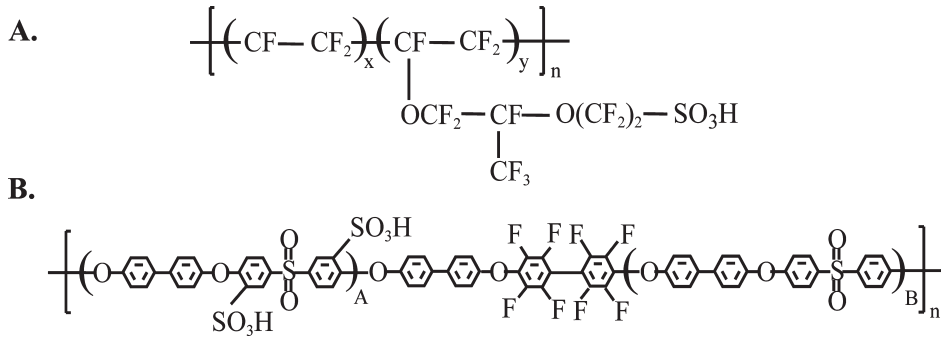

Figure 1. (A) Chemical structure of Nafion, where (*x*:*y*) represents the ratio of hydrophobic to hydrophilic part. (B) Chemical structure of BPSH−BPS multiblock copolymers, where A and B represent the hydrophilic and hydrophobic block masses, respectively.

the hydrophilic channels in the ionomers. Thus, the diffusion and partial alignment behavior can be considered as a reflection of the intrinsic characteristics of the materials. In this paper, we report systematic studies of water diffusion and anisotropy for a series of aromatic hydrocarbon multiblock copolymers, both of which varied substantially over a range of water uptakes. We observe uptake-dependent and block-length-dependent diffusion anisotropy for these copolymers. ^{2}H NMR spectroscopy on these materials, which measures partial ordering of absorbed D_2O molecules through their quadrupole splittings, reflects the alignment of the polymer matrix as well as changes in hydrophilic channel dimensions. This distinct alignment information, on a different length scale than diffusion measurements, correlates with diffusion anisotropy. These two techniques combined provide insight into average defect and domain structures in these materials, specifically from the standpoint of water transport.

2. Experimental Section

2.1. Membrane Preparation and Properties. Nafion NRE212 (dispersion cast) membrane with equivalent weight of 1100 (grams of dry membrane per mole of sulfonate group) and thickness of 50 μm was purchased from E.I. Dupont in the acid form. The multiblock copolymers named as BPSH−BPS (A:B) were obtained from Prof. James E. McGrath's group, and the synthetic procedures have been reported elsewhere.[2] The chemical structures are shown in Figure 1. Similar to Nafion, these multiblock copolymers contain two parts, with A and B representing the block masses of hydrophilic and hydrophobic parts individually, and are coupled with the linkage group of decafluorobiphenyl (DFBP). For the materials presented in this work, the block masses range from 3 to 15 kg/mol, and in all cases A = B. As reported elsewhere,[13] all these block copolymers were redissolved in *N*-methyl-2-pyrrolidinone (NMP, Fisher), followed by solution casting onto a clean glass substrate. The prepared films were cast under an infrared lamp with temperature controlled between 45 and 55 °C for 2 days. Membranes were further dried in a vacuum oven at 110 °C for a whole day to remove the residual solvent. For acidification, membranes were boiled in 0.5 M sulfuric acid for 2 h and then rinsed and boiled in deionized water. Dry membrane thicknesses were 30−40 μm. Depending on membrane type and uptake, this value increased to 60−100 μm upon water swelling.

2.2. Water Uptake Control. A key issue in diffusion measurements is the water content in the membrane. Making measurements relevant to relative humidity is often set up as a standard parameter for operating fuel cells since it is easy to control. However, a drawback lies in the fact that the actual amount of water in the membrane may fluctuate during cell operation, and this water uptake directly determines membrane transport properties. To solve this problem, we developed several specially designed Teflon cells. Membranes were cut into pieces of 5.5 mm × 5 mm in size, stacked together to a total mass

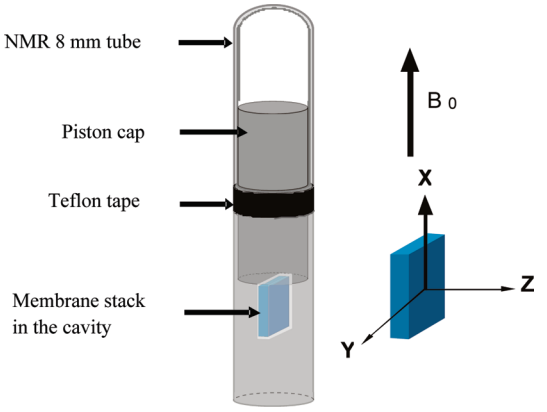

Figure 2. Sealed Teflon cell configuration. Membrane pieces are stacked in the same orientation to snugly fit the rectangular shaped cavity in the cell. A piston cap is used to seal the cell in which membranes are equilibrated. An NMR tube is connected to the piston cap for ease of handling, and the sample cavity is centered in the NMR coil.

of ~40 mg, and trimmed to match the rectangular shaped cavity in the cell, as shown in Figure 2. Thus, dead volume is only ~20% of membrane stack volume. A piston cap seals the cell in order to control the water uptake. An 8 mm NMR tube connects to the piston cap with Teflon tape wrapped around at the junction of the two, so as to rigidly fix the sample cell in the bore of the NMR probe. In this way, we locate the samples at the center of the NMR detection coil. Stacks of membranes were not dried in an oven but in a desiccator overnight at room temperature (~25 °C) to avoid any possible heating history effect. Later, membranes were soaked in H_2O for at least 24 h. The wet membranes were blotted to remove free surface water and transferred to the sealed Teflon cell to equilibrate for a period of 8−12 h. All the diffusion measurements were performed at 25 °C after sample equilibration. Masses of wet membranes were determined gravimetrically after the NMR experiment. Water uptake is calculated using eq 1:

$$\text{water uptake} = \frac{\text{mass}_{\text{wet}} - \text{mass}_{\text{dry}}}{\text{mass}_{\text{dry}}} \times 100\% \qquad (1)$$

2.3. Diffusion Anisotropy Measurement by Pulsed-Field-Gradient NMR. We apply the robust and simple pulsed-gradient stimulated echo sequence (PGSTE)[18] for all diffusion measurements. ^1H_2O diffusion in the membrane was measured using a Bruker Avance III WB 400 MHz (9.4 T) NMR equipped with a Micro5 triple-axis-gradient microimaging probe and 8 mm double resonance (^{1}H/^{2}H) rf coil. The triple axis gradients each have a maximum value of 300 G/cm and were employed here in three orthogonal directions relative to the membranes, identified as *X*, *Y*, and *Z* in Figure 2. Orientation of the

Table 1. Sample Properties and NMR Relaxation Times.

sample ID	block mass (kg/mol)	water uptake (%)	T_1 range (ms)	T_2 range (ms)
BPSH−BPS(3k−3k)	3	11−24	9−12	2.5−3.2
BPSH−BPS(5k−5k)	5	16−31	9−12	2.9−3.5
BPSH−BPS(10k−10k)	10	16−62	6−20	1.5−4.9
BPSH−BPS(15k−15k)	15	15−41	7−17	2.0−4.7
Nafion 212	EW = 1.1	9−22	24−50	7.0−16

membrane stacks in the magnetic field were verified using a $Y-Z$ image slice collected with a RARE pulse sequence. The PGSTE sequence used a $\pi/2$ pulse time of 32 μs, gradient pulse durations (δ) ranging from 1 to 2 ms, and diffusion times (Δ) ranging from 7 to 20 ms, depending on the specific material (see Table 1). 32 gradient steps were applied, and the maximum gradient strength was selected to produce 70%−90% NMR signal attenuation. Because of differences in water uptake, the number of scans varied from 8 to 256 to produce sufficient signal-to-noise-ratio for each data point. All parameters for the gradient have been calibrated and optimized as reported earlier.[3] As shown in Figure 2, X and Y are two orthogonal directions parallel to the membrane plane while the Z direction is perpendicular to the membrane plane. Correspondingly, the measured self-diffusion coefficient is marked as D_{xx}, D_{yy}, and D_{zz} ($D_\perp$). The diffusion anisotropy factor is defined as $S_D = D_\parallel/D_\perp$, where $D_\parallel$ is the average value of the in plane values D_{xx} and D_{yy}. Using the sealed cell and triple axis gradient, we can interrogate diffusion along any direction to probe diffusion tensorial properties (anisotropy) without readjusting the membranes orientation. This feature greatly enhances the accuracy and reliability of the measurements.

2.4. ^{2}H NMR Spectroscopy. ^{2}H NMR experiments were performed additionally to observe orientational ordering in the ionomers. This technique can assist in determining the alignment modes of materials with anisotropic structures.[3,19,22] Single pulse experiments ($\pi/2$ = 20 μs) were performed with repetition time of 0.5 s and number of scans ranging from 256 to 1024, depending on D_2O uptake. The studied materials were soaked in D_2O (99.9%, Cambridge Isotope Laboratories) with the measured uptake ranging from 6 to 20 wt %. Home-built Teflon cells similar to Figure 2 were utilized with one having an additional configuration to allow orientation of membrane stacks either vertically or horizontally with respect to the magnetic field. These cells were placed inside the above-described imaging probe and rf coil. Relevant detailed procedures are summarized in our previous report.[3] Deuterium quadrupole splittings $\Delta\nu_Q$ were obtained by fitting each spectrum with two Lorentzian peaks using NutsPro software (Acorn NMR Inc., Livermore, CA).

3. Results and Discussion

3.1. Sealed Sample Cell: Stable NMR Measurements on Water-Swollen Membranes. Figure 3 clearly illustrates the effectiveness of using the sealed cell. When a membrane is placed into a regular NMR tube, the measured diffusion coefficient (solid symbols) decreases linearly over the "equilibration" time. This phenomenon is due to water in the membranes evaporating into the space around the sample, resulting in the continual decrease of water diffusion. This same effect is seen in capped tubes, but to a lesser extent. In contrast, using our sealed cell (open symbols), and after 1 h equilibration time, one observes no change in the measured diffusion coefficient over hours or even days, which demonstrates the function of our sealed cell in obtaining repeatable experiments.

3.2. Diffusion vs Water Uptake. Since both T_1 and T_2 decrease with water uptake, and considering the limits they place on the PGSTE sequence, relevant experiment variables, such as diffusion time (Δ) and gradient pulse duration (δ), are properly selected ($\Delta < 1.5T_1$, $\delta < T_2$) to ensure sufficient signal-to-noise ratio and diffusion signal attenuation. For a given sample, higher water uptake samples exhibit longer T_1 and T_2 (see Table 1). Following these conditions, Figure 4 shows the results of in-plane diffusion ($D_\parallel$) measurements vs water uptake. In order to further assess membrane transport and defect structure, we attempted to probe restricted diffusion over a range of Δ. At high water uptake (40−60%), D does not vary with Δ in the range of 10−30 ms (T_1 and T_2 limited) for any of these materials. At low water uptake, however, due to hardware (imaging probe) limitations (g_{max} = 300 G/cm) as well as the short T_1 and T_2 values, the range of Δ cannot be varied substantially above 10 ms. For all materials, water diffusion coefficients monotonically increase with water uptake. Among the block copolymers, BPSH−BPS (10k−10k) exhibited the best water transport, which we attribute to its ordered morphology and high connectivity among hydrophilic domains.[2] Here, the length scale probed by the NMR diffusion measurement can be estimated via calculating the root-mean-square displacement of a molecule undergoing

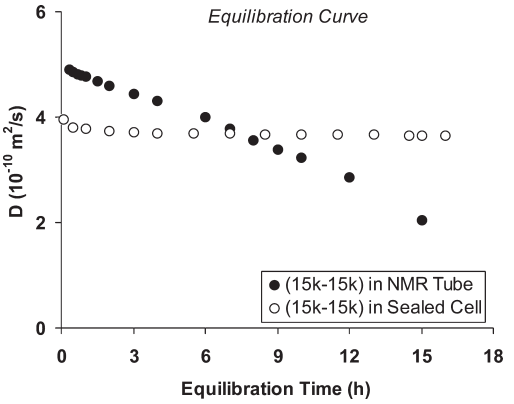

Figure 3. Water self-diffusion coefficient (D) in BPSH−BPS (15k−15k) measured vs equilibration time. D decreasesd over time if membranes were put in an open NMR tube (solid); D was fairly constant over the whole equilibration time with use of the sealed Teflon cell.

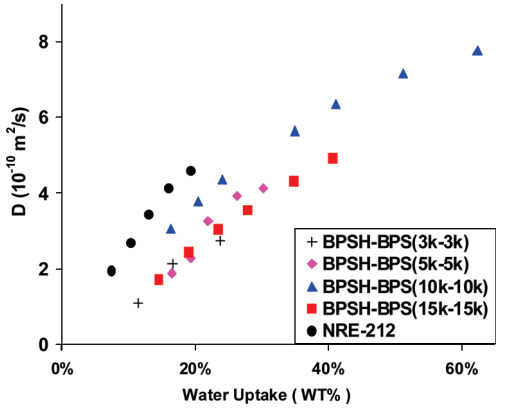

Figure 4. Plots of water diffusion in plane ($D_\parallel$) vs water uptake. Results allow for comparison of water diffusion vs water uptake among different materials. Error bars are within the size of each data point.

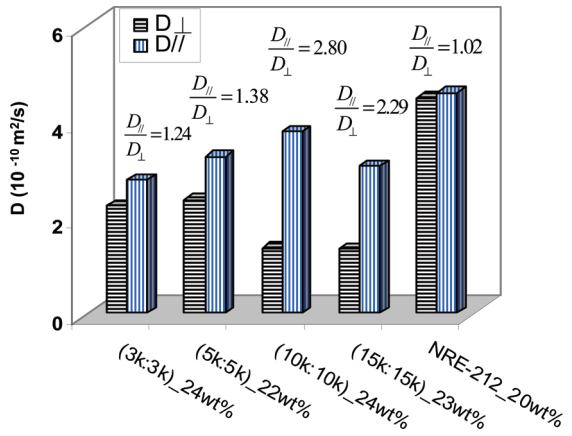

Figure 5. Illustration of diffusion anisotropy vs membrane type: $D_\perp$ (through-plane); $D_\parallel$ (in-plane). At nearly the same water uptake, diffusion anisotropy dramatically varies with membrane type. Nafion 212 exhibits isotropic diffusion while BPSH−BPS (10k−10k) shows the maximum anisotropy in diffusion. (Error bar is estimated to be 3% of the value of each data column.)

a 1D random walk: $\langle r^2\rangle^{1/2} = (2D\Delta)^{1/2}$, where D is the diffusion coefficient and Δ is the diffusion time in the PGSTE pulse sequence. In the case of BPSH−BPS (10k−10k), for instance, where $D_\parallel$ varies from 3×10^{-10} to 8×10^{-10} m^2/s, we find that the diffusion length $\langle r^2\rangle^{1/2}$ ranges from 2.5 to 4 μm (Δ = 10 ms). In addition, at nearly the same water uptake, the water self-diffusion coefficient for BPSH−BPS (5k−5k) is lower than that for BPSH−BPS (10k−10k) but slightly higher than that for BPSH−BPS (15k−15k). This indicates that the water transport in these membranes does not monotonically increase with block length, suggesting an optimum morphology or defect structure vs molecular weight. We also note that the 10k−10k material has a much larger saturation value of the water uptake, allowing faster overall diffusion than the other block lengths or Nafion 212. However, when comparing at equivalent water uptake values, N212 attains the fastest water diffusion. The higher saturation water uptakes of the 10k−10k and 15k−15k materials also reflect a different (planar) morphology than the others,[2] which becomes more apparent in the next section.

3.3. Diffusion Anisotropy. We observe diffusion anisotropy, defined as the ratio of $D_\parallel$ to $D_\perp$, ranging from 1.02 to 2.80 in the different materials at ~22 wt % uptake (see Figure 5). Water diffusion in Nafion 212 behaves nearly isotropically as we reported earlier.[3] For the block copolymers, $D_\parallel/D_\perp$ increases with block mass but again reaches a maximum for 10k−10k. More importantly, $D_\parallel/D_\perp$ increases by only 15% as the block mass increased from 3k to 5k, whereas the value increases by >100% as the block mass increases from 5k to 10k. This large enhancement in diffusion anisotropy implies a transition in morphology since water diffusion reflects the symmetry of such structures. This speculation is further supported by results of diffusion anisotropy vs water uptake for the different materials as illustrated in Figure 6. In general, water diffusion is nearly isotropic for Nafion and only somewhat anisotropic for low block mass copolymers (3k−3k, 5k−5k). In addition, the ratio $D_\parallel/D_\perp$ shows no dependence on water uptake in these three cases. This phenomenon most likely originates from similar morphological symmetries intermediate between 3D and 2D, giving rise to predominantly 3D elastic constraints in these materials, the presence of which does not allow preferential contraction or expansion of hydrophilic channels in any specific direction. Thus, $D_\parallel$ and $D_\perp$ would be affected similarly, and their ratio stays constant.

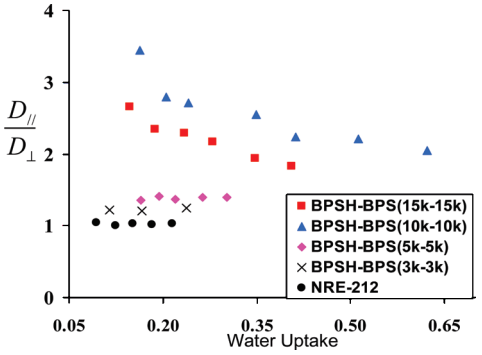

Figure 6. Diffusion anisotropy ($D_\parallel/D_\perp$) of different materials plotted vs water uptake. For (3k−3k) and (5k−5k) copolymers as well as Nafion 212, $D_\parallel/D_\perp$ has no dependence on uptake. For (10k−10k) and (15k−15k), $D_\parallel/D_\perp$ is large and decreases with uptake.

In contrast, $D_\parallel/D_\perp$ has a strong inverse dependence on water uptake for high block mass copolymers (10k−10k and 15k−15k). This phenomenon provides further evidence for the existence of a uniform planar (lamellar) structure globally within these block copolymers, which also exhibits agreement with the local TEM pictures,[16] wherein layers are stacked through the plane. As a result, the corresponding 3D elastic constraints would be drastically reduced, resulting in a quasi-2D symmetry with less rigidity in the through-plane dimension. Such a configuration will lead to substantial growth of layer spacings with water uptake, which also correlates with anisotropic swelling results.[13] In the presence of higher amounts of water swollen into the membrane, water molecules should experience fewer restrictions as they diffuse through the plane due to the improved connectivity among hydrophilic channels, and furthermore these faster diffusing water molecules should sample a larger average number of defects with pathways through the lamellar planes. However, with reduced water uptake, the smaller diffusion length probed by the water molecules during the measurement time Δ makes it less likely for water molecules to access routes to transport through the plane, thus leading to enhanced diffusion anisotropy.

3.4. Probing Alignment with ^{2}H Spectroscopy. To further inform our understanding of anisotropy in these materials, we examined them via quadrupole splittings ($\Delta\nu_Q$) observed in ^{2}H NMR spectroscopy on absorbed D_2O.[3,22] Figure 7 shows ^{2}H spectra from membrane stacks oriented in three orthogonal directions along the magnetic field. The broad line widths in these spectra are due to the intrinsic properties of these materials rather than spectrometer field inhomogeneity. This line width may arise from a combination of two possible factors: (1) homogeneous T_2 line broadening due to fundamental D_2O−matrix interactions or (2) distributions of domain orientations where the domains are larger than the diffusion length the molecules sample during the experimental time scale ($1/\Delta\nu_Q$).

Single component ^{2}H line shapes (two line spectra) are observed in all membranes with maximum splittings $\Delta\nu_Q$ when B_0 is along Z (through-plane), thus revealing that these materials are uniformly macroscopically aligned with a symmetry axis (director) perpendicular to the membrane plane. At the same uptake, we observed that peak splitting increases as block mass increases, which represents the enhancement of ordering within the materials. The splittings in the other two in-plane directions are similar to each other, and their values are close to half of the maximum splittings. These results exhibit the same pattern as observed in Nafion 212,[22] indicating that the block copolymers are aligned

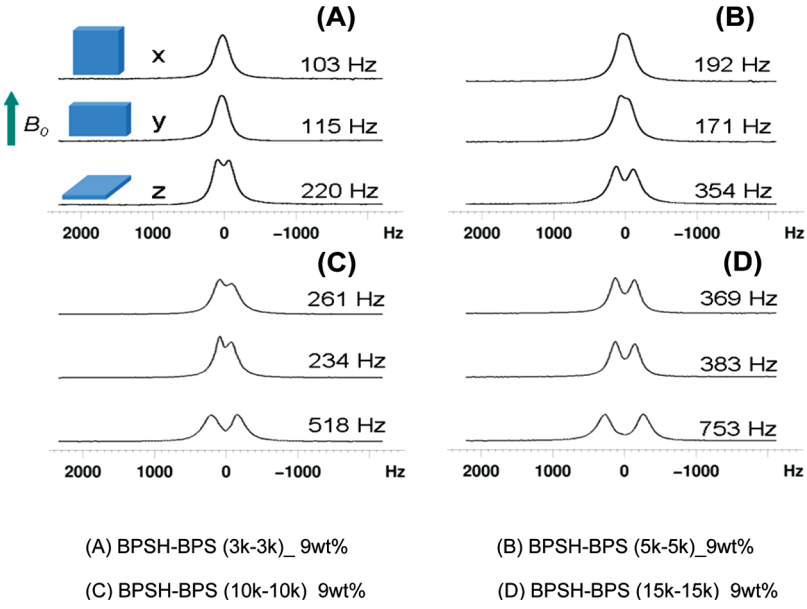

Figure 7. Room temperature ^{2}H spectra of BPSH−BPS multiblock copolymers vs block mass and at fixed D_2O uptake. Stacks of membranes were oriented in three orthogonal directions along the magnetic field B_0. Maximum peak splitting $\Delta\nu_Q$ is observed when the membrane plane is perpendicular to B_0 (Z direction). Minimum splitting is observed when B_0 is parallel to the orientation of the membrane plane (X or Y). Maximum splittings are approximately twice the values of the minimum splittings.

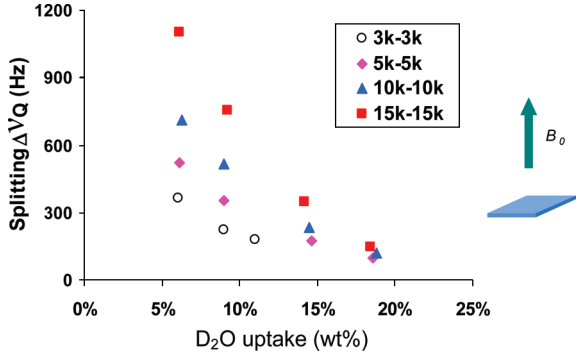

Figure 8. Room temperature (25 °C) ^{2}H splitting vs D_2O uptake for block copolymers, with membrane stacks oriented perpendicular to B_0. Splitting increases dramatically with block mass. Error bars are within the size of each data point.

uniaxially, as would be expected for cast membranes, and which can be described by eq 2[3]

$$\Delta\nu_Q = \frac{1}{2}\Delta\nu_0[3\cos^2\theta - 1 + \eta\sin^2\theta] \qquad (2)$$

where $\Delta\nu_0$ is the maximum splitting observed for these materials (Z-aligned) and θ is defined as the angle between material alignment axis with respect to the magnetic field direction. η is the biaxiality parameter, and it is equal to zero for uniaxially aligned structures. In the present case, we attribute the small nonzero biaxialities ($\eta < 0.06$) to variations in both film casting conditions and to small errors in peak fitting due to the broad line widths observed.

Figure 8 lists the results of ^{2}H splittings through the plane vs D_2O uptake. We attribute the strong inverse dependence of splitting on uptake, especially for high block mass copolymers, as arising from expansion of the hydrophilic channels with water, causing these highly mobile water molecules to experience on average more interactions with other (nearly isotropic) water molecules and fewer anisotropic "confinement interactions" with the channel walls. A striking result lies in that the largest splittings occur for the highest block mass, which contradicts the trend of diffusion anisotropy. We discuss this mystery in the next section.

3.5. Length Scales of Anisotropy and Defect Structure. Considering that both water diffusion and ^{2}H splitting measurements will reflect the anisotropy of a specific material, one notices an apparently contradictory pattern when comparing Figure 6 to Figure 8, where the anisotropy of 10k−10k is the highest in the former case but lower than 15k-15k in the latter. To propose an answer to this intriguing question, we will discuss three factors which will mainly contribute to the anisotropy in materials: tilt angle distribution of hydrophilic domains, domain size, and defects (density, distribution, etc.). Our explanation to this paradox is aided by the illustrations in Figure 9, based on electron micrographs for similar materials.[16] We assert that the 10k−10k copolymer possesses more tilted domains, containing fewer dead ends (defects and layer plane tilt reversals) along the in-plane direction. On the other hand, 15k−15k possesses more uniformly oriented domains with more dead ends at length scales below the diffusion length, but on the same or larger scale than the ^{2}H spectroscopy measurement length scale (replace Δ with $1/\Delta\nu_Q$ in the random walk expression of section 3.2 to get ~0.4 μm). From this point of view, in terms of diffusion, water molecules will on average experience less barriers in plane for 10k−10k to give an enhanced diffusion anisotropy. In contrast, with respect to ^{2}H spectroscopy, which is sensitive to the global ordering (average of local ordering) of a material but probes a smaller length scale, it is reasonable that although 15k−15k contains more dead ends, it will exhibit larger quadrupole splittings due to its more uniformly aligned lamellar structure. In other words, as the dotted circle scans through the whole picture of Figure 9A,B to average over the local ordering, one would expect to obtain a higher splitting value for 15k−15k, given the fact that more local domains are aligned along the director. The structures in Figure 9 are somewhat exaggerated to illustrate these points, which form a cohesive (if not infallible) explanation of our results. Thus, the combination of diffusion anisotropy and ^{2}H spectroscopy provide distinct

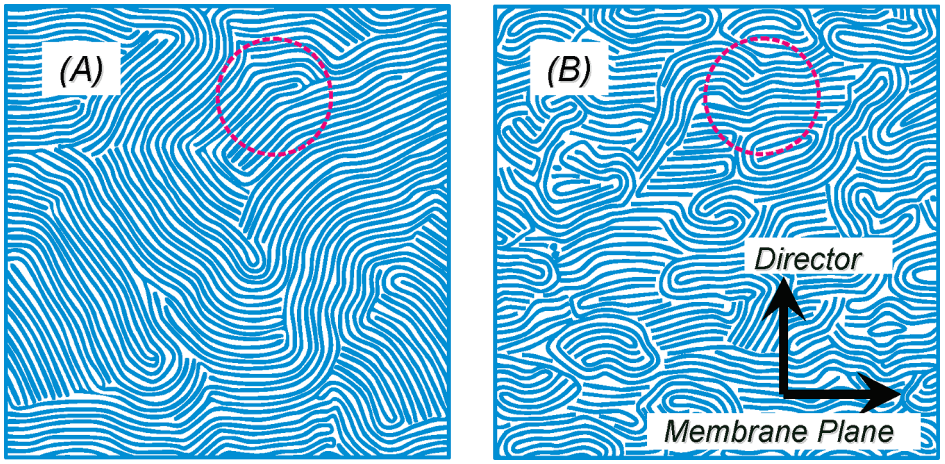

Figure 9. Illustrative models of morphologies for 10k−10k (A) and 15k−15k (B) based on NMR diffusion and ^{2}H spectroscopy results. The director on average is perpendicular to the membrane (and lamellar layer) plane, as indicated by the black arrows. The dotted circle serves to represent the average length scale that D_2O molecules sample during the spectroscopy experiments (~0.4 μm), thus reflecting more local alignment qualities. The diffusion experiments probe substantially larger length scales (~4 μm), comparable to the size of these pictures. On the basis of these NMR results, we conclude that, compared to 10k−10k, the average local ordering is higher in 15k−15k, resulting in less variation in domain tilt angles thus larger ^{2}H splittings, while the defect structure has higher density resulting in lower diffusion anisotropy and slower in plane diffusion. Note layer spacings ~30 nm from TEM.[16]

yet complementary information regarding the symmetry of morphological anisotropy and transport on different length scales and time scales.

Additionally, in view of the TEM images[16] where the average layer spacing may vary in the range of 20−40 nm depending on uptake, one should also note the low value of $D_{\|}/D_{\perp}$ in our measurements, which should be higher by at least an order of magnitude as expected for similar materials with very few defects.[27,28] That is, we attribute these reasonably low anisotropy results to the distribution of defects (dislocations and disclinations), the presence of which not only provide pathways for water molecules to transport perpendicular to the lamellae but also become dead ends to reduce $D_{\|}$. It is quite conceivable that these materials can be controlled further in terms of synthesis and processing in order to minimize defects and improve anisotropy. Indeed, the methods described here provide a quantitative mechanism for feedback on such materials optimization. We are additionally working toward application of diffusion−diffusion correlation spectroscopy (DDCOSY)[29] to further probe the local as well as global anisotropy with the purpose of building a well-defined physical model that can describe how defects (density, distribution, type, etc.) will affect the diffusion and anisotropy in these and related materials.

4. Conclusions

We have performed systematic studies of water diffusion and anisotropy on a class of hydrocarbon multiblock copolymers as well as on Nafion 212. Both diffusion in-plane and through-plane have been measured and compared for all materials. Various levels of diffusion anisotropy were observed in all the multiblock copolymers, where water diffusion in plane was faster than through plane. In contrast, no anisotropy of diffusion was observed in Nafion 212. For Nafion 212 and low block mass copolymers (3k, 5k), $D_{\|}/D_{\perp}$ has no dependence on water uptake over the accessible range. However, a strong dependence of $D_{\|}/D_{\perp}$ on water uptake was observed in the high block mass copolymers (10k, 15k), which corroborates the existence of macroscopically aligned lamellae parallel to the membrane plane. ^{2}H NMR spectroscopy further demonstrates macroscopically ordered lamellar structures aligned uniaxially with symmetry axis through the membrane plane. The combination of these two methods, each probing a different length scale in the materials, gives quantitative insight into domain sizes, domain alignments, and defect distributions. Further developments of these ideas and applications of these methods will provide a broader and deeper picture of how transport relates to morphology in ionomer membranes.

Acknowledgment. The authors graciously thank Professor James E. McGrath and Dr. Hae-Seung Lee for providing block copolymer samples and relevant information and discussions. This material is based upon work supported by the National Science Foundation under Award DMR 0844933. Any opinions, findings and conclusions, or recommendations expressed in this material are those of the author(s) and do not necessarily reflect the views of the National Science Foundation (NSF). This material is based upon work supported in part by the U.S. Army Research Office under Grant W911NF-07-1-0452 Ionic Liquids in Electro-Active Devices (ILEAD) MURI. Acknowledgment is made to the Donors of the American Chemical Society Petroleum Research Fund for partial support of this research and to Virginia Tech for startup funds.

References and Notes

(1) Rahardianto, A.; Gao, J. B.; Gabelich, C. J.; Williams, M. D.; Cohen, Y. *J. Membr. Sci.* **2007**, *289*, 123–137.
(2) Roy, A.; Lee, H. S.; McGrath, J. E. *Polymer* **2008**, *49*, 5037–5044.
(3) Li, J.; Wilmsmeyer, K. G.; Madsen, L. A. *Macromolecules* **2009**, *42*, 255–262.
(4) Schmidt-Rohr, K.; Chen, Q. *Nat. Mater.* **2008**, *7*, 75–83.
(5) Gierke, T. D.; Munn, G. E.; Wilson, F. C. *J. Polym. Sci., Part B: Polym. Phys.* **1981**, *19*, 1687–1704.
(6) Samms, S. R.; Wasmus, S.; Savinell, R. F. *J. Electrochem. Soc.* **1996**, *143*, 1498–1504.
(7) Sone, Y.; Ekdunge, P.; Simonsson, D. *J. Electrochem. Soc.* **1996**, *143*, 1254–1259.
(8) White, H. S.; Leddy, J.; Bard, A. J. *J. Am. Chem. Soc.* **1982**, *104*, 4811–4817.
(9) Zawodzinski, T. A.; Derouin, C.; Radzinski, S.; Sherman, R. J.; Smith, V. T.; Springer, T. E.; Gottesfeld, S. *J. Electrochem. Soc.* **1993**, *140*, 1041–1047.
(10) James, P. J.; Elliott, J. A.; McMaster, T. J.; Newton, J. M.; Elliott, A. M. S.; Hanna, S.; Miles, M. J. *J. Mater. Sci.* **2000**, *35*, 5111–5119.
(11) Mehta, V.; Cooper, J. S. *J. Power Sources* **2003**, *114*, 32–53.
(12) Kim, Y. S.; Wang, F.; Hickner, M.; McCartney, S.; Hong, Y. T.; Harrison, W.; Zawodzinski, T. A.; McGrath, J. E. *J. Polym. Sci., Part B: Polym. Phys.* **2003**, *41*, 2816–2828.

(13) Lee, H. S.; Roy, A.; Lane, O.; Dunn, S.; McGrath, J. E. *Polymer* **2008**, *49*, 715–723.
(14) Hickner, M. A.; Ghassemi, H.; Kim, Y. S.; Einsla, B. R.; McGrath, J. E. *Chem. Rev.* **2004**, *104*, 4587–4611.
(15) Wang, H.; Badami, A. S.; Roy, A.; McGrath, J. E. *J. Polym. Sci., Part A: Polym. Chem.* **2007**, *45*, 284–294.
(16) Badami, A. S.; Lane, O.; Lee, H. S.; Roy, A.; McGrath, J. E. *J. Membr. Sci.* **2009**, *333*, 1–11.
(17) Stejskal, E. O.; Tanner, J. E. *J. Chem. Phys.* **1965**, *42*, 288.
(18) Tanner, J. E. *J. Chem. Phys.* **1970**, *52*.
(19) Deloche, B.; Samulski, E. T. *Bull. Am. Phys. Soc* **1981**, *26*, 327–328.
(20) Johnson, C. S. *Prog. Nucl. Magn. Reson. Spectrosc.* **1999**, *34*, 203–256.
(21) Price, W. S. *Concepts Magn. Res.* **1997**, *9*, 299–336.
(22) Li, J.; Wilmsmeyer, K. G.; Madsen, L. A. *Macromolecules* **2008**, *41*, 4555–4557.
(23) Gong, X.; Bandis, A.; Tao, A.; Meresi, G.; Wang, Y.; Inglefield, P. T.; Jones, A. A.; Wen, W. Y. *Polymer* **2001**, *42*, 6485–6492.
(24) Ohkubo, T.; Kidena, K.; Ohira, A. *Macromolecules* **2008**, *41*, 8688–8693.
(25) Rollet, A. L.; Blachot, J.; Delville, A.; Diat, O.; Guillermo, A.; Porion, P.; Rubatat, L.; Gebel, G. *Eur. Phys. J. E* **2003**, *12*, S131–S134.
(26) Kidena, K. *J. Membr. Sci.* **2008**, *323*, 201–206.
(27) Hamersky, M. W.; Tirrell, M.; Lodge, T. P. *Langmuir* **1998**, *14*, 6974–6979.
(28) Wasterby, P.; Oradd, G.; Lindblom, G. *J. Magn. Reson.* **2002**, *157*, 156–159.
(29) Callaghan, P. T.; Furo, I. *J. Chem. Phys.* **2004**, *120*, 4032–4038.